Metallurgy and Foundry Engineering – Vol. 41, 2015, No. 4, pp. 181–188
http://dx.doi.org/10.7494/mafe.2015.41.4.181

**Łukasz Rakoczy, Lechosław Tuz, Krzysztof Pańcikiewicz**

# Hot cracking of nickel-based superalloy turbine blade

## Pękanie gorące łopatki turbiny z nadstopu na osnowie niklu

**Abstract**
The aim of this study was to present the hot cracking behavior of a blade originating from a turbine blade segment. The crack was induced by a gas tungsten arc welding process, and the research material was a MAR-M247 nickel based superalloy. This alloy is considered to be difficult to weld because of its high tendency to crack. Light microscopy and scanning electron microscopy show the occurrence of cracking in the melted zone, heat-affected zone, and base alloy. A scanning electron microscopy investigation revealed that cracks are propagated by stresses and liquation of the low temperature constituent.

**Keywords:** superalloys, nickel alloys, liquation, hot cracking, turbine blades

**Streszczenie**
Celem pracy była analiza mikrostrukturalna pęknięcia gorącego na powierzchni łopatki z segmentu van cluster. Pęknięcie powstało w wyniku oddziaływania skoncentrowanego źródła ciepła, jakim był łuk elektryczny jarzący się w osłonie argonu. Łopatka została wykonana z nadstopu na osnowie niklu o nazwie handlowej MAR-M247. W przypadku konwencjonalnych metod spawania jest on uważany za trudno spawalny. Przeprowadzono badania makrostruktury i mikrostruktury za pomocą mikroskopii świetlnej i skaningowej. Na podstawie wykonanych badań stwierdzono występowanie pęknięć ciągłych zarówno w obszarze przetopionym, strefie wpływu ciepła, jak i materiale rodzimym. Obserwacje za pomocą skaningowej mikroskopii elektronowej pozwoliły na stwierdzenie, że pęknięcie propagowało w wyniku naprężeń, jak również likwacji niskotopliwych składników mikrostruktury.

**Słowa kluczowe:** nadstopy, stopy niklu, likwacja, pękanie gorące, łopatki turbiny

## 1. Introduction

One of the materials that the Martin Marietta company developed in the 1970s is polycrystalline nickel-based superalloy MAR-M247. Its good castability, corrosion resistance

**Łukasz Rakoczy M.Sc. Eng., Lechosław Tuz Ph.D. Eng., Krzysztof Pańcikiewicz M.Sc. Eng.:** AGH University of Science and Technology, Faculty of Metals Engineering and Industrial Computer Science, Krakow, Poland; lrakoczy@agh.edu.pl

at high temperatures, and high mechanical properties (including creep strength) made it a widely used alloy in gas turbine structures. Its combination of unique properties contributed to MAR-M247's use for rotating components in aircraft engines, including turbine blades and segments [1, 2]. Strengthening of the alloy mainly corresponds with semicoherent precipitation γ′. MAR-M247 is comprised of about a 60% volume of intermetalic phase $Ni_3$(Al, Ti). Additional solution strengthening is due to the presence of Co, Mo, W, and Cr. Carbon, boron, zirconium, and hafnium precipitate mainly in the form of carbides and borides along the grain boundaries (which improves creep strength). The increased amount of refractory metals (i.e., Ta, W, and Mo) as well as the aforementioned Hf and the segregation of alloying elements during crystallization lead to the formation of the eutectic γ/γ′ and carbides in the interdendritic regions [3–5]. Due to the considerable differences in their chemical composition and the resulting differences in their structural composition, the welding of nickel-based superalloys is difficult. Elements in the alloys may take on slightly different roles that may cause difficulties related to the attainment of good-quality welds or pad welds. The properties of nickel alloys in the aerospace industry require the use of special welding and repair technology. The high cost of nickel superalloys as well as development in welding technology have compelled the aviation industry to repair rather than replace such components after long-term service or even utilize new parts with casting defects that are in need of repair. For this purpose, welding technologies such as cladding and brazing are often used. Manufacturers of aircraft engines have accurately defined the requirements of repair-welding technologies [6–8]. The scope of this study is to present the repair results of the MAR-M247 nickel alloy.

## 2. Experimental procedure

The component used in these experiment was cast the turbine segment presented in Figure 1. The lement is made of the nickel-based superalloy known as MAR-M247. The chemical composition of the alloy is given in Table 1. The first stage of our investigation was to characterize the base metal microstructure. Subsequently, the airfoil of the blade was modified by Gas Tungsten Arc Welding. For this purpose, an Oerlikon welding machine was used. The parameters of the GTAW process are presented in Table 2. For light microscopy, the sample was initially ground with sandpaper (with weights of #320, #600, #800, #1000, #1200, and #2000) and then mechanically polished with diamond paste of 3 μm and 1 μm grits. Afterwards, the sample was electrolytically etched with a 10% solution of chromium (VI) trioxide. The investigation was carried out on a Leica light microscope. The scanning electron microscopy (SEM) examination and energy dispersive spectroscopy were conducted on a Jeol microscope operated at 20 kV. Imaging in the SEM was performed by backscattered electrons on the polished samples.


*Fig. 1. Turbine segment originating from aircraft engine*

*Table 1. Chemical composition of MAR-M247 [3]*

| Element | Co | W | Cr | Al | Ta | Hf | Ti | Mo | C | Zr | B | Ni |
|---|---|---|---|---|---|---|---|---|---|---|---|---|
| % wt. | 10 | 10 | 8.4 | 5.5 | 3 | 1.5 | 1 | 0.7 | 0.15 | 0.05 | 0.015 | Bal. |

*Table 2. Parameters of regeneration by GTAW*

| Current [A] | Voltage [V] | Travel speed [mm/min] | Efficiency η | Heat input [kJ/cm] |
|---|---|---|---|---|
| 50 | 12 | 240 | 0.65 | 0.97 |

# 3. Results and discussion

## 3.1. Microstructural characterization of base metal

The microstructure and EDS spectrum of nickel based superalloy MAR-M247 are presented in Figure 2.

a) b)

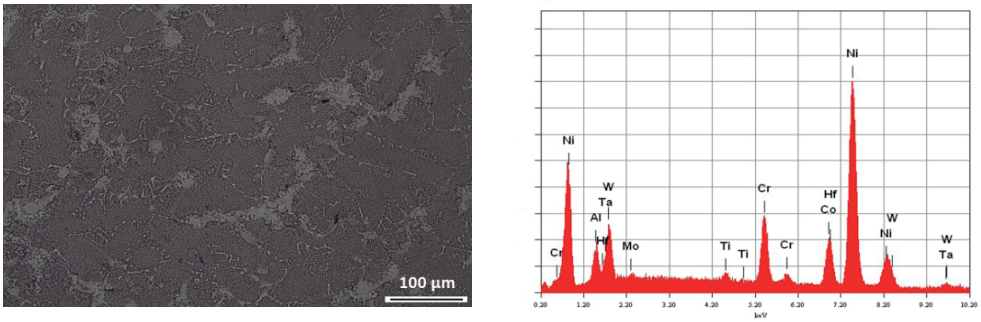


*Fig. 2. Cast MAR-M247: a) microstructure; b) EDS spectrum*

The microstructure revealed equiaxed grains in the blade-as-cast and after heat treatment (Fig. 2a). The obtained microstructures show that the analyzed MAR-M247 originated from a low-pressure turbine. Different methods of casting such elements allows to reached directionally solidified structure for use in the high-pressure turbine [1]. Further observations of the microstructures using a higher magnification and the EDS spectrum of carbide are presented in Figure 3.

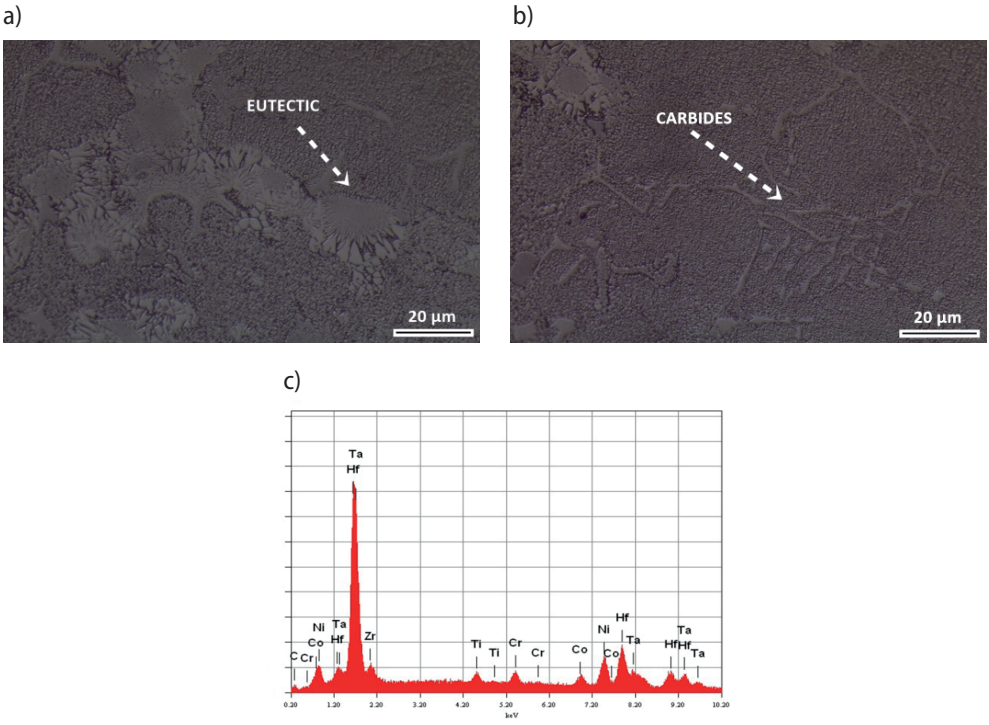


*Fig. 3. Precipitation in as-received condition: a) eutectic; b) carbides; c) EDS spectrum of carbide.*

It obtained that carbides as well as eutectic γ/γ′ are revealed (Figs. 3a, 3b). In the microstructure, $M_{23}C_6$-, $M_6C$-, and MC-type carbides can be present [2]. Evidence of an MC-type carbide (Hf, Ta)C was confirmed during energy dispersive spectroscopy (Fig. 3c).

## 3.2. Microstructure of hot cracking

The typical macrostructure of the observed cracking is presented in Figure 4.

In the macrostructure (Fig. 4a), a crack was observed over the entire width of the melted region. The crack did not stop at the fusion line; as a result, liquation of the grain boundary and high stress expanded in the direction of the base material through the heat-affected zone (Figs. 4b, 4c).

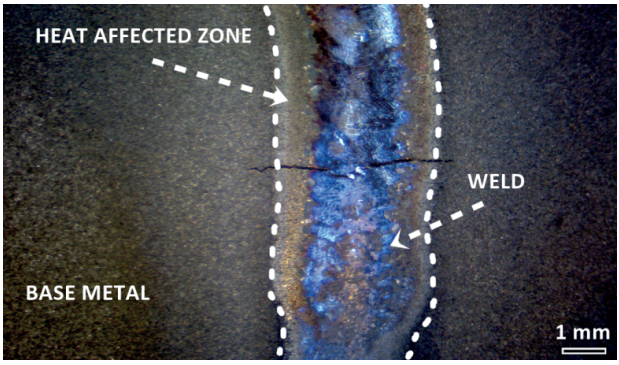


*Fig. 4. General location of crack obtained during repair welding*

As a result of welding, the width of the melted area is just over 2 mm (Fig. 5a), while the heat-affected zones are about 600 µm (Figs. 5b, 5c). The dimension of the crack in the base metal is shown in Figure 6.

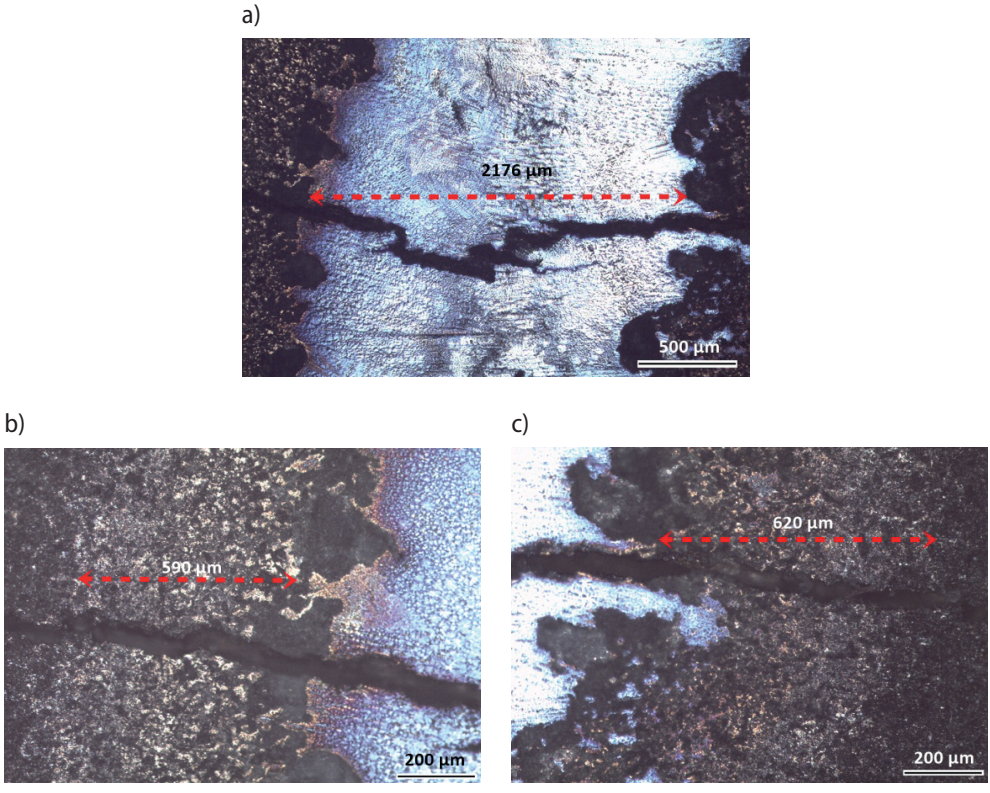


*Fig. 5. Dimension of investigated regions: a) melted region; (b, c) HAZ*

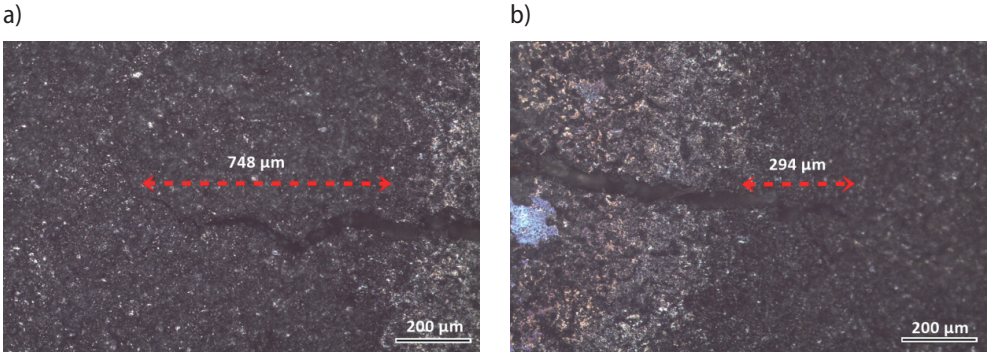


*Fig. 6. Length of crack in base metal: a) left side; b) right side*

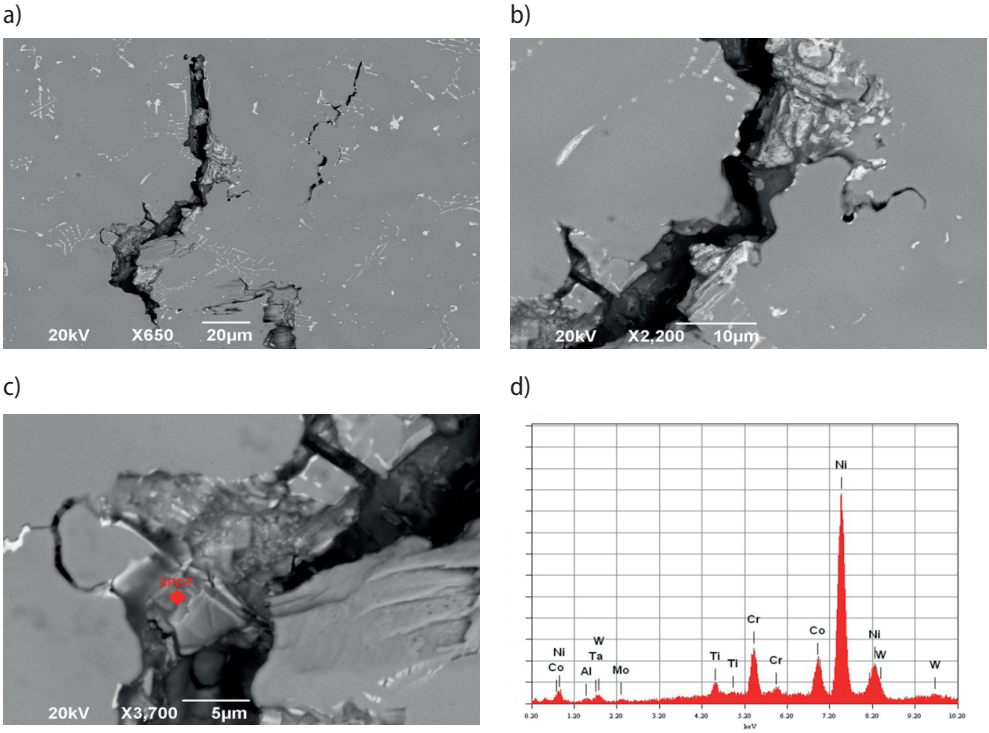


*Fig. 7. Microstructure of crack: a) general view; b) liquated carbides; c) location of EDS spot; d) EDS spectrum*

On the left side, the crack developed into the base metal through 748 µm (Fig. 6a), and so the total length of the crack (HAZ and BM) on this side is about 1350 µm. On the other side, the crack is shorter – only about 915 µm (Fig. 6b). The difference in the crack's dimensions is probably the result of different heat conductivity in the base metal near

the tip and on the opposite side. The crack on the right side is located near the leading edge, and so the higher cooling rate did not allow it to propagate a greater distance into the base metal (the thickness of the base metal near the leading edge is lower). Figures 7 and 8 illustrate more details about the microstructure of the crack.

An SEM investigation allows us to state that the crack propagated in close proximity to the carbides and eutectic (Fig. 7a). The solidus temperature of the base material is higher than the incipient melting temperature of the eutectic and carbides; so, liquid was present during the welding process along the grain boundaries (Fig. 7b). The thermal stresses and melted constituents caused failure and did not allow us to repair the component. The energy dispersive x-ray spectroscopy analysis shows that the selected area cracked near eutectic γ/γ′ (Figs. 7c, 7d).

a) b)

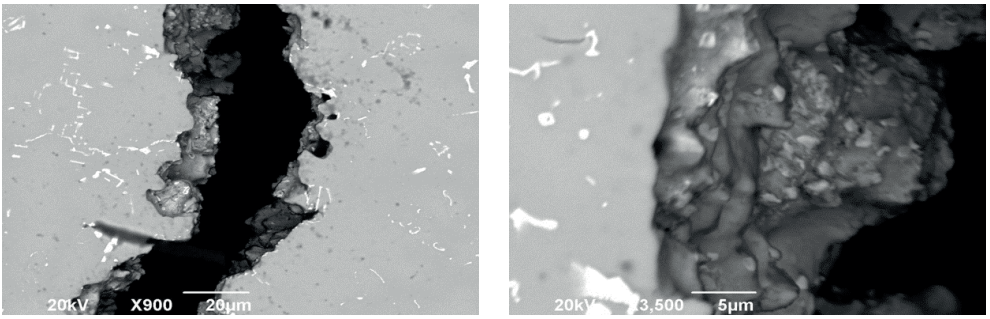


*Fig. 8. Change of crack microstructure: a) increased width; b) fracture with carbide precipitates*

The greater temperature gradient and increased stresses contributed to the change in the crack's microstructure. The crack in the selected region was wider, while on the edges, the base metal was fully melted (Fig. 8). Figure 8b illustrates the fracture of hot crack and primary carbide precipitates with diameters of about 1 µm.

## 4. Discussion of cracking mechanism

Due to their complex chemical composition, alloys melt and solidify at a wide range of temperatures. This range is expanded with increasing amounts of alloying elements, and for nickel-based superalloys, this range is quite wide. Hot cracking is initiated in the final stage of crystallization of the weld. A liquid film along the grain boundaries and closed in the interdendritic spaces at a sufficiently high level of stress, resulting in the low ability of a material to strain (ultimately leading to cracking). The metal surrounding the weld also begins to shrink due to the cooling that increases the level of stress. In the welding process, the base material adjacent to the fusion line is heated up to a temperature within the range of solidus-liquidus. The microstructure in this region is partially melted

and, thus, is described as the partially melted zone (PMZ). Cracking occurs in the PMZ because the liquid distributed along the grain boundaries cannot accommodate stresses. The sensitivity of a weld on hot cracking is determined by both metallurgical factors and local stress levels in the final stage of crystallization. The tendency of nickel-based superalloys to hot cracking is greater with the increase of heat input.

## 5. Summary

The results show the high tendency of nickel-based superalloy MAR-M247 to hot cracking. This is associated both with the chemical composition resulting from the high contents of titanium and aluminum (Al + Ti > 6 wt.%) a well as the used welding process. Due to its relatively high heat input, gas tungsten arc welding is not appropriate to repair these types of elements. The increased heat input caused a high level of stress, so the crack expanded through both the melted region and heat-affected zone to the base metal. The length of the crack indicates that the repair of these types of components must be performed using a concentrated heat source such as a plasma arc or laser beam. The selection of parameters should be taken into account for reducing welding stresses and the liquation of low melting temperature constituents.

## Acknowledgements

This research work was supported by the Polish Ministry of Science and Higher Education, Grant No. 11.11.110.299.

### References

[1] Roskosz S.: Kompleksowa ocena porowatości odlewów precyzyjnych z żarowytrzymałych nadstopów niklu. Wydawnictwo Politechniki Śląskiej, Gliwice 2011
[2] Azevedo e Silva P.R.S., Baldan R., Nunes C.A., Coelho G.C., da Silva Costa A.M.: Solution heat-treatment of Nb-modified Mar-M247 superalloy. Materials Characterization, 75 (2013), 214–219
[3] Baldan R., Rocha R., Tomasiello R.: Solutioning and aging of MAR-M247 nickel-based superalloy. Journal of Materials Engineering and Performance, 22, 9 (2013), 2574–2579
[4] Li Z., Gobbi Q S.L., Richter K.H.: Autogenous welding of Hastelloy X to Mar-M 247 by laser. Journal of Materials Processing Technology, 70 (1997), 285–292
[5] Szczotok A., Rodak K.: Microstructural studies of carbides in MAR-M247 nickel-based superalloy. Materials Science and Engineering, 35 (2012), 1–11
[6] Kou S.: Solidification and liquation cracking issues in welding. The Journal of The Minerals, Metals & Materials Society, 55 (2003), 37–42
[7] Klimpel A., Kik T., Mazur Ł.: Żarowytrzymałe stopy niklu – skład chemiczny i struktura. Biuletyn Instytutu Spawalnictwa, 4 (2009), 66–72
[8] Klimpel A., Rzeźnikiewicz A.: Technologia naprawy uchwytów klapy dużej biernej silnika odrzutowego RD-33. Przegląd Spawalnictwa, 9 (2011), 43–49